# Interacting scales and triad enstrophy transfers in generalized two-dimensional turbulence

Watanabe, Takeshi

Iwayama, Takahiro

# Interacting scales and triad enstrophy transfers in generalized two-dimensional turbulence

Takeshi Watanabe*
*Graduate School of Engineering, Department of Engineering Physics, Nagoya Institute of Technology, Gokiso, Showa-ku, Nagoya 466-8555, Japan*
*and CREST, Japan Science and Technology Agency, 4-1-8 Honcho, Kawaguchi, Saitama 332-0012, Japan*

Takahiro Iwayama†
*Department of Earth and Planetary Sciences, Graduate School of Science, Kobe University, Kobe 657-8501, Japan*
(Received 7 June 2007; published 3 October 2007)

The local and nonlocal characteristics of triad enstrophy transfer in the enstrophy inertial range of generalized two-dimensional turbulence, so-called $\alpha$ turbulence, are investigated using direct numerical simulations, with a special emphasis on $\alpha=1$, 2, and 3. The enstrophy transfer via nonlocal triad interactions dominates the transfer dynamics in the enstrophy inertial range, irrespective of $\alpha$. However, the contributions from more local interactions to the total enstrophy transfer increase as $\alpha$ decreases. The results are discussed in connection with the local and nonlocal transition of the enstrophy transfer at $\alpha=2$ expected from the phenomenological scaling theory. The specific nature of the enstrophy transfer in surface quasigeostrophic turbulence ($\alpha=1$) is also discussed.

DOI: 10.1103/PhysRevE.76.046303 PACS number(s): 47.27.ek, 47.27.Gs, 92.60.hk

## I. INTRODUCTION

The energy and enstrophy in two-dimensional (2D) Navier-Stokes (NS) turbulence are transferred in a peculiar manner. The former is transferred toward larger scales, while the latter is transferred toward smaller scales. We expect that the enstrophy spectrum in the enstrophy inertial range (EIR) obeys a power law of the form $Q(k)\sim k^{-1}$ by applying a local similarity theory for the energy cascade in three dimensions (3D) [1] to the enstrophy cascade in the EIR. This is known as Kraichnan-Leith-Batchelor (KLB) scaling [2–4]. The underlying physical picture of the energy cascade in 3D is that the energy transfer occurs between similar scales, i.e., the local interactions are dominant for energy transfer in the inertial range. The success of the KLB theory depends on the nature of the enstrophy transfer between the interacting scales. Previous theoretical and numerical studies have demonstrated that the contribution from nonlocal interactions to the enstrophy transfer is more important than that from local interactions [5–12], suggesting the sensitivity of statistics in the EIR scales to variations in the large-scale conditions.

The local and nonlocal characteristics of enstrophy transfer have been explored in the studies of a generalized 2D turbulence, so-called $\alpha$ turbulence [13–16]. The governing equation of motion of $\alpha$ turbulence is given by

$$\frac{\partial q}{\partial t}+\mathbf{u}\cdot\boldsymbol{\nabla}q=D+F, \tag{1}$$

$$q_{\mathbf{k}}=-|\mathbf{k}|^{\alpha}\phi_{\mathbf{k}}, \tag{2}$$

where $q(\mathbf{r},t)$ is a scalar field convected by the velocity field $\mathbf{u}=-\nabla\times\phi\mathbf{e}_z$, $\phi$ is the stream function, and $q_{\mathbf{k}}$ and $\phi_{\mathbf{k}}$ are the coefficients of a Fourier series expansion of $q$ and $\phi$, respectively. The terms $D$ and $F$ represent the dissipation term acting on both large and small scales and the external forcing, respectively. $\alpha$ turbulence is characterized by the relationship (2) between $q$ and $\phi$ with a single real parameter $\alpha$. For certain values of $\alpha$, Eqs. (1) and (2) reduce to the evolution equation for some well-known 2D turbulent systems [32].

Equation (1) has two quadratic positive invariants called the *energy* $E_\alpha=-\langle q\phi/2\rangle$ and the *enstrophy* $Q_\alpha=\langle q^2/2\rangle=\int_0^\infty Q_\alpha(k)dk$ when $D=F=0$. The enstrophy spectrum $Q_\alpha(k)$ in the EIR,

$$Q_\alpha(k)\sim k^{-(7-2\alpha)/3}, \tag{3}$$

has been derived theoretically by applying the KLB theory to $\alpha$ turbulence [13]. Direct numerical simulations (DNSs) of $\alpha$ turbulence have been used to demonstrate that the results for $0<\alpha<2$ are close to the form (3), while the scaling law (3) is not supported by DNS for $\alpha>2$. The scaling law

$$Q_\alpha(k)\sim k^{-1} \tag{4}$$

has been observed irrespective of $\alpha$ [13,14]. Thus, previous studies have shown a "phase transition of the spectral slope," suggesting a drastic change in the transfer dynamics at $\alpha=2$.

Pierrehumbert *et al.* [13] and Schorghofer [14] have emphasized the importance of nonlocal interactions in the enstrophy transfer responsible for the failure of the KLB theory when $\alpha>2$ by invoking an analogy to the passive scalar transport. Recently, we developed their ideas by incorporating nonlocal effects into the KLB theory of $\alpha$ turbulence, in which a unified form of the enstrophy spectrum was used to explain the phase transition of the spectral slope at $\alpha=2$ [16]. This spectrum was derived as

$$Q_\alpha(k)\sim \eta_\alpha^{2/3}k^{-(7-2\alpha)/3}[\chi_\alpha^+(k)]^{-1/3}, \tag{5}$$

*watanabe@nitech.ac.jp
†iwayama@kobe-u.ac.jp

 

$$\chi_\alpha^+(k) = \frac{1}{4-2\alpha}\left[1 - \{1-(4-2\alpha)\chi_\alpha^+(k_1)\}\left(\frac{k_1}{k}\right)^{4-2\alpha}\right], \quad (6)$$

where $k_1$ is the smallest wave number in the EIR. Note that the function $\chi_\alpha^+(k)$ gives a large-scale correction to the KLB scaling due to nonlocal effects. Equations (5) and (6) are a naive generalization of the scaling theory for the 2D NS turbulence proposed by Kraichnan [5] and Bowman [6] to $\alpha$ turbulence. As shown in [16], the unified form of Eqs. (5) and (6) precisely explains the local and nonlocal transition at $\alpha=2$, i.e., the asymptotic form of Eqs. (5) and (6) with $k \gg k_1$ is reduced to the KLB scaling (3) when $\alpha<2$, while Eq. (4) is obtained irrespective of $\alpha$ in the range $k \gg k_1$ when $\alpha > 2$. This scaling form is in good agreement with DNS results, as will be demonstrated in Sec. III.

The above scaling theory is based on the assumption that the nonlocal nature is phenomenologically incorporated into the effective rate of shear acting on $k$ as

$$\omega_\alpha(k) = \left(\int_0^k k'^{4-2\alpha} Q_\alpha(k')dk'\right)^{1/2}, \quad (7)$$

which is the key to success of the unified scaling theory [16]. However, this dimensional evaluation is heuristic because the role of nonlocal interactions in the actual enstrophy transfer is not clear at present. It should be emphasized that the detailed nature of contributions from local or nonlocal interactions to the enstrophy transfer must be examined by analyzing the bare transfer function that arises from the nonlinear term of the governing equation of motion. Up to now, many studies have examined the importance of nonlocal interactions on the triad enstrophy transfer in the EIR of 2D NS turbulence [7,8,11]. To our knowledge, however, no study has discussed the detailed characteristics of the enstrophy transfer in $\alpha$ turbulence from the point of view of the interacting scales and triad enstrophy transfer.

The main purpose of the present paper is to clarify the local or nonlocal characteristics of $\alpha$-turbulence enstrophy transfer by performing DNSs for several positive $\alpha$ cases. We investigated the features of the interacting scales that accompany the enstrophy transfer by computing the triad transfer function originating from the nonlinear term of the governing equation of motion. Contributions to the enstrophy transfer from the local or nonlocal triad interactions are discussed by decomposing the transfer functions and transfer fluxes into components containing the degree of the interacting scales. We also reconsider the potential of the phenomenological scaling theory responsible for the success of the local and nonlocal transition at $\alpha=2$ based on our DNS results and discuss the specific nature of the enstrophy transfer for $\alpha=1$, i.e., for surface quasigeostrophic (SQG) turbulence.

This paper is organized as follows. Section II presents the DNS formulation and the method used to analyze statistical quantities such as the triad transfer function and the transfer fluxes. The DNS results are presented and discussed in Sec. III. The results are compared to the phenomenological scaling theory to determine the spectral behavior for the range $\alpha>0$ in Sec. IV. Our conclusions are summarized in Sec. V.

## II. FORMULATION

### A. DNS conditions

We numerically integrated the governing equation for the scalar field $q(\mathbf{x},t)$ in a periodic square with periodicity $2\pi$, which is given in wave number space by

$$\left(\frac{\partial}{\partial t} + d_{\mathbf{k}}^S + d_{\mathbf{k}}^L\right) q_{\mathbf{k}} = \sum_{\mathbf{l}} \sum_{\mathbf{m}} S_\alpha(\mathbf{l},\mathbf{m}) q_{\mathbf{l}}^* q_{\mathbf{m}}^* \delta_{\mathbf{k}+\mathbf{l}+\mathbf{m},0} + f_{\mathbf{k}}, \quad (8)$$

$$S_\alpha(\mathbf{l},\mathbf{m}) = \frac{1}{2}(\mathbf{l}\times\mathbf{m})_z\left(\frac{1}{|\mathbf{m}|^\alpha} - \frac{1}{|\mathbf{l}|^\alpha}\right), \quad (9)$$

where $d_{\mathbf{k}}^S$ and $d_{\mathbf{k}}^L$ are the dissipation terms, $f_{\mathbf{k}}$ is the forcing term, and $q_{\mathbf{k}}^*$ is the complex conjugate of $q_{\mathbf{k}}$. We used hyperviscosity to dissipate the enstrophy at small scales, $d_{\mathbf{k}}^S = -\nu_{2p}k^{2p}$ with degree $p=4$, and a drag force $d_{\mathbf{k}}^L=-\nu_0$ within the wave-number range $|\mathbf{k}|\leqslant 2$ to remove the accumulating energy at large scales. The external forcing $f_{\mathbf{k}}$, imposed to maintain steady turbulence, was chosen from $f_{\mathbf{k}} = A\exp[i\psi_{\mathbf{k}}(t)]$ with a constant amplitude $A$ and a uniform random phase $\psi_{\mathbf{k}}(t)$ in $\mathbf{k}$ and time, which has a spectral support at the wave-number band $1\leqslant|\mathbf{k}|\leqslant 2$. We focused our interest on the special cases of $\alpha=1,2$, and 3. A pseudospectral method was used for the DNSs, which were performed with $N^2=1024^2$ spatial grid points and a cutoff wave number $k_c=[N/3]$, $[\cdots]$ as a Gaussian symbol. To ensure the convergence of the statistical quantities, temporal averages were taken over a large duration of time until we obtained clear plateaus of the enstrophy transfer flux with the same value as the enstrophy dissipation rate $\eta_\alpha$ when plotted on a linear scale. The detailed numerical scheme and DNS parameters can be found in our previous paper [16].

### B. Definition of the statistical quantities

The statistical quantities used to discuss the nature of the enstrophy transfer of $\alpha$ turbulence are presented in this section. The spectral balance equation was derived from Eq. (8) as

$$\left(\frac{\partial}{\partial t} + 2d_{\mathbf{k}}^S + 2d_{\mathbf{k}}^L\right) Q_\alpha(k,t) = T_\alpha^Q(k,t) + F_\alpha(k,t), \quad (10)$$

where the enstrophy spectrum $Q_\alpha(k,t)$ is defined by

$$Q_\alpha(k,t) = \sum_{\mathbf{k}}{}' \frac{1}{2}\langle|q_{\mathbf{k}}|^2\rangle. \quad (11)$$

The angle brackets denote an ensemble average. The summation $\Sigma_{\mathbf{k}}'$ is taken over a cylindrical shell region with a radius $k$ and width $\Delta k=1$. The term $F_\alpha(k,t)$ originates from the external forcing $f_{\mathbf{k}}$ in Eq. (8). Hereafter, the ensemble average is replaced by a temporal average, as performed in conventional DNS studies for steady turbulence, so that the time argument can be omitted. The enstrophy transfer function $T_\alpha^Q(k)$ can be expressed in terms of the triad enstrophy transfer function $T_\alpha^Q(k|l,m)$ as

$$T_\alpha^Q(k) = \sum_{l=0}^{\infty}\sum_{m=0}^{\infty} \frac{1}{2} T_\alpha^Q(k|l,m), \quad (12)$$

$$T_\alpha^Q(k|l,m) = \sum_{\mathbf{k}}{}' \sum_{\mathbf{l}}{}' \sum_{\mathbf{m}}{}' 2S_\alpha(\mathbf{l},\mathbf{m}) \mathrm{Re}\langle q_{\mathbf{k}}^* q_{\mathbf{l}}^* q_{\mathbf{m}}^* \rangle \delta_{\mathbf{k+l+m},0}, \tag{13}$$

where Re denotes the real part of a complex number. The triad transfer function satisfies the detailed balance equations corresponding to the existence of two quadratic positive invariants when $d_{\mathbf{k}}^{L,S}=f_{\mathbf{k}}=0$. For the enstrophy,

$$T_\alpha^Q(k|l,m) + T_\alpha^Q(l|m,k) + T_\alpha^Q(m|k,l) = 0, \tag{14}$$

and for the energy,

$$\frac{T_\alpha^Q(k|l,m)}{k^\alpha} + \frac{T_\alpha^Q(l|m,k)}{l^\alpha} + \frac{T_\alpha^Q(m|k,l)}{m^\alpha} = 0. \tag{15}$$

Equations (14) and (15) lead to

$$\frac{T_\alpha^Q(k|l,m)}{T_\alpha^Q(l|m,k)} = \frac{l^{-\alpha} - m^{-\alpha}}{m^{-\alpha} - k^{-\alpha}}, \tag{16}$$

$$\frac{T_\alpha^Q(l|m,k)}{T_\alpha^Q(m|k,l)} = \frac{m^{-\alpha} - k^{-\alpha}}{k^{-\alpha} - l^{-\alpha}}, \tag{17}$$

$$\frac{T_\alpha^Q(m|k,l)}{T_\alpha^Q(k|l,m)} = \frac{k^{-\alpha} - l^{-\alpha}}{l^{-\alpha} - m^{-\alpha}}. \tag{18}$$

The enstrophy transfer flux is defined by

$$\Lambda_\alpha(k) = -\sum_{k'=0}^{k} T_\alpha^Q(k') = \sum_{k'=k}^{\infty} T_\alpha^Q(k'). \tag{19}$$

In the statistically steady state, the value of $\Lambda_\alpha(k)$ in the EIR is independent of $k$ and equals the enstrophy dissipation rate $\eta_\alpha$ given by

$$\eta_\alpha = 2\nu_p \sum_{k=0}^{\infty} k^{2p} Q_\alpha(k). \tag{20}$$

The enstrophy transfer flux (19) can be decomposed into two components using Eqs. (14) and (15):

$$\Lambda_\alpha(k) = \Lambda_\alpha^+(k) + \Lambda_\alpha^-(k), \tag{21}$$

where the functions $\Lambda_\alpha^+(k)$ and $\Lambda_\alpha^-(k)$ are defined by

$$\Lambda_\alpha^+(k) = \frac{1}{2} \sum_{k'>k} \sum_{l<k} \sum_{m<k} T_\alpha^Q(k'|l,m), \tag{22}$$

$$\Lambda_\alpha^-(k) = -\frac{1}{2} \sum_{k'<k} \sum_{l>k} \sum_{m>k} T_\alpha^Q(k'|l,m). \tag{23}$$

$\Lambda_\alpha^+(k)$ is the net enstrophy input into all wave numbers $>k$ from the interactions with $l$ and $m$ both $<k$, while $\Lambda_\alpha^-(k)$ is the net enstrophy input into all wave numbers $<k$ from the interactions with $l$ and $m$ both $>k$.

### C. Computation of the triad transfer function

To obtain detailed information about the transfer dynamics in wave-number space, we must compute Eq. (13) for all triads within the numerical spatial resolution limitations and determine its behavior for variations in all combinations of $k$, $l$, and $m$. However, such a computation is too expensive, even with modern computers. Therefore, in the present study, we evaluated a coarse-grained triad transfer function that maintained the physical relevance of the original triad transfer function instead of computing Eq. (13) directly from the DNS data. The coarse-graining procedure was as follows. We divided the wave-number space into circular logarithmic shells so that the summation with respect to $\mathbf{k}$ in wave-number space was divided into two operations,

$$\sum_{\mathbf{k}} = \sum_{n=0}^{N_c} \sum_{k_n \leqslant |\mathbf{k}| < k_{n+1}}, \tag{24}$$

where $k_n$ is the shell wave number labeled by index $n$ as

$$k_n = k_0 \lambda^n, \tag{25}$$

and $N_c$ is the cutoff shell number defined by $N_c = [\log_\lambda(k_c/k_0)]$. Thus, the representative shell wave number was set to be equidistant on a logarithmic scale, where the shell $n$ has a radius of $k_n$ and contains the wave numbers of modulus $k$ from $k_n$ to $k_{n+1}$.

We represented the statistical quantities defined in the previous subsection in terms of the shell indices. The coarse-grained triad transfer function $T_\alpha^Q(n|a,b)$ can be defined by

$$T_\alpha^Q(n|a,b) = \sum_{k_n \leqslant |\mathbf{k}| < k_{n+1}} \sum_{l_a \leqslant |\mathbf{l}| < l_{a+1}} \sum_{m_b \leqslant |\mathbf{m}| < m_{b+1}} 2S_\alpha(\mathbf{l},\mathbf{m}) \times \mathrm{Re}\langle q_{\mathbf{k}}^* q_{\mathbf{l}}^* q_{\mathbf{m}}^* \rangle \delta_{\mathbf{k+l+m},0}, \tag{26}$$

where the circular shells are represented by $k_n=k_0\lambda^n$, $l_a=l_0\lambda^a$, and $m_b=m_0\lambda^b$, with $\{n,a,b\}=0,1,\ldots,N_c$. Thus, $T_\alpha^Q(n|a,b)$ represents the mean enstrophy transfer among three shells, labeled as $(n,a,b)$. $T_\alpha^Q(k)$ and $\Lambda_\alpha(k)$ are represented in terms of the shell indices as

$$T_\alpha^Q(n) = \sum_{a=0}^{N_c} \sum_{b=0}^{N_c} \frac{1}{2} T_\alpha^Q(n|a,b), \tag{27}$$

$$\Lambda_\alpha(n) = -\sum_{n'=0}^{n-1} T_\alpha^Q(n') = -\sum_{n'=0}^{n-1} \sum_{a=0}^{N_c} \sum_{b=0}^{N_c} \frac{1}{2} T_\alpha^Q(n'|a,b). \tag{28}$$

We set the parameters $k_0$ and $\lambda$ to $k_0=1$ and $\lambda=\sqrt{2}$, respectively, so that the index $n$ varied from $n=0$ to $N_c=16$ for the present DNS resolution.

The computational cost to evaluate (26) can be reduced significantly using fast Fourier transforms (FFTs) when computing the coarse-grained nonlinear term in Eq. (8). Similar approaches have been used in previous DNS studies of NS turbulence in 2D [7,8] and in 3D [25,26].

## III. DNS RESULTS

### A. Enstrophy inertial range spectra

First, we examined the existence of the EIR in our simulations. Figure 1 shows the enstrophy transfer flux $\Lambda_\alpha(n)$

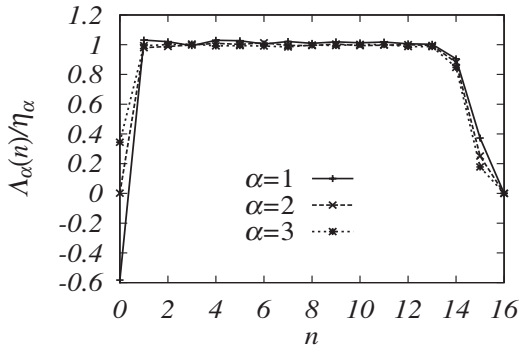


FIG. 1. Variations in the enstrophy transfer fluxes for $\alpha=1$, 2, and 3 against the shell index $n$.

normalized by the enstrophy dissipation rate $\eta_\alpha$ plotted against the shell index $n$ for $\alpha=1$, 2, and 3. Plateaus were observed between $2\leqslant n\leqslant 13$, irrespective of $\alpha$. Thus, we shall call this wave-number range as the EIR, irrespective of $\alpha$. The shells for $n=0$ and 1 correspond to the wave-number range in which the external and drag forces act, while the shells for $n=14-16$ correspond to the dissipation range due to hyperviscosity.

The compensated enstrophy spectrum in terms of the KLB scaling (3) is plotted in Fig. 2 for $\alpha=1$, 2, and 3. The deviation from the KLB scaling law is more significant with increasing $\alpha$. For $\alpha=1$, the present DNS results indicate a less steep behavior than the KLB scaling in the range $4\leqslant\log_\lambda k\leqslant 11$ (almost corresponding to the range $5\leqslant k\leqslant 50$). In previous DNS observation, the spectral slope in the EIR for $\alpha=1$ was slightly steeper than $k^{-5/3}$ [13,14] due to dissipation effects. This less steeper spectrum is in sharp contrast to previous DNS studies. To test the validity of the form of Eq. (5), we also plotted the function (6) representing the large-scale correction to the KLB scaling due to nonlocal effects, in which the parameters included in $\chi_\alpha^+(k)$ were numerically determined by curve fitting the modeled transfer flux [16]. The manner in which our results deviated from the KLB scaling was well represented by $\chi_\alpha^+(k)^{-1/3}$ in the range $5\leqslant k\leqslant 50$ for all cases of $\alpha$. For $50<k$, the spectral slope for

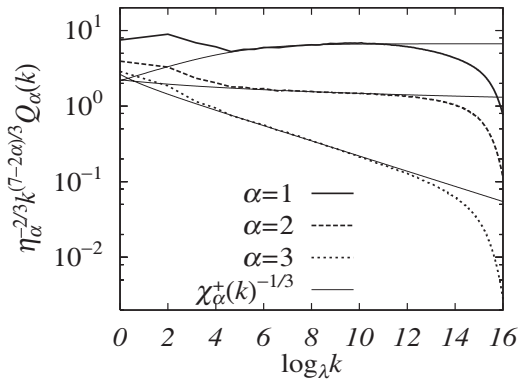


FIG. 2. Behavior of the compensated enstropy spectra $\eta_\alpha^{-2/3}k^{(7-2\alpha)/3}Q_\alpha(k)$ for $\alpha=1$, 2, and 3. The reference thin lines give the prediction from Eq. (5) with Eq. (6), in which the included parameters are evaluated using the curve-fit form of the modeled transfer flux; see [16] for details.

$\alpha=1$ still deviated from $k^{-5/3}$. This steeper spectrum may be indicative of insufficient resolution in our simulation because the spectral slopes for $\alpha=2$ and 3 in this range are also steeper than the predictions from Eq. (5). Therefore, the unified scaling law (5) works very well for both $\alpha\geqslant 2$ and $\alpha<2$ systems, as discussed in our previous paper [16]. The less steeper spectral slope for $\alpha=1$ in the wave-number range $5\leqslant k\leqslant 50$ suggests that the nonlocal effects are significant even for $\alpha=1$ in this range. In fact, this point will be shown in the following sections.

We comment on the asymptotic behavior of $\chi_\alpha^+(k)$ when $\alpha=2$. We obtain $\chi_2^+(k)=\ln(k/k_1)+\chi_2^+(k_1)$ from Eq. (6) in the limit $\alpha\to 2$, where a constant $\chi_2^+(k_1)$ is given by $\chi_2^+(k_1)\sim\eta_2^{-1}\omega_2(k_1)^3$ [16]. When $\chi_2^+(k_1)$ is much larger than $\ln(k/k_1)$ in the EIR of $k$, which is realized when there exists a huge bump in $Q_2(k)$ of the forcing wave-number range $(k<k_1)$ [12], we evaluate $\omega_2(k_1)\sim Q_2^{1/2}$. Therefore the asymptotic behavior of the enstrophy spectrum is derived from Eqs. (5) and (6) as $Q_2(k)\sim\eta_2 Q_2^{-1/2}k^{-1}$, which is consistent with a nonuniversal spectrum in the EIR suggested in [12]. This represents that the logarithm-corrected spectrum by Eqs. (5) and (6) (with $\alpha=2$) unifies the original logarithm-corrected form derived by [5] and a nonuniversal scaling form suggested by [12].

### B. Behavior of the triad enstrophy transfer function

We investigated the coarse-grained triad transfer function defined in the previous section to discuss the characteristics of the enstrophy transfer between interacting scales in the EIR. Contour plots of $T_\alpha^Q(n|a,b)$ normalized by $\eta_\alpha$ are shown in Figs. 3 ($n=3$), 4 ($n=8$), and 5 ($n=13$) for each value of $\alpha$. The thin curved lines plotted in each figure represent boundaries due to the triad interaction limitations between the wave vectors as $\mathbf{k}+\mathbf{l}+\mathbf{m}=\mathbf{0}$. The triad transfer function $T_\alpha^Q(n|a,b)$ is permitted to have values inside these curves, although their boundaries are not rigorous due to the coarse-graining procedure. The contour levels in each figure are the same so we can discuss the characteristics of the enstrophy transfer for different $n$. Even though the detailed behavior of the enstrophy transfer depends on $n$, even when $n$ is in the EIR, significant findings can be observed from Figs. 3–5.

(1) The triad enstrophy transfer function $T_\alpha^Q(n|a,b)$ reached a maximum or minimum at $(n,a,b)=(n,n-1,0)$ $[(n,0,n-1)]$ or $(n,a,b)=(n,n+1,0)$ $[(n,0,n+1)]$. Therefore, the enstrophy transfer via the forcing scale shells is the dominant transfer process in these systems, as shown previously for 2D NS turbulence [8,9]. This trend is independent of $\alpha$ and $n$ in the EIR.

(2) The amplitudes of $T_\alpha^Q(n|n-1,0)$ and $T_\alpha^Q(n|n+1,0)$ for fixed $n$ in the EIR increased with $\alpha$. Therefore, the amount of net enstrophy transfer via the extreme nonlocal interaction is more dominant in the EIR for the larger $\alpha$ case. The enstrophy transfer occurs almost entirely between the two modes with similar scales, while the other mode corresponds to the forcing scales.

(3) The enstrophy transfer via more local interactions, such as $T_\alpha^Q(n|n+1,n-1)$, grew as $\alpha$ decreased when $n$ was

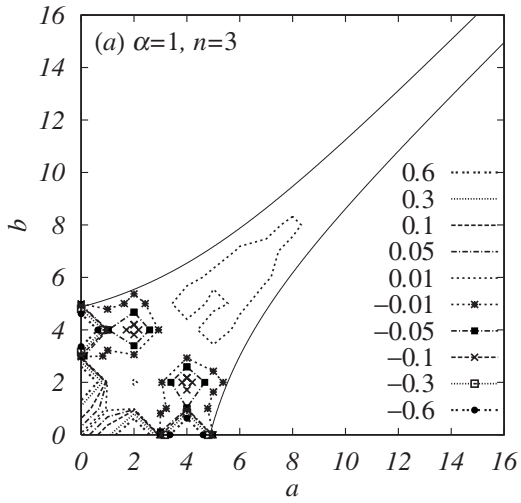


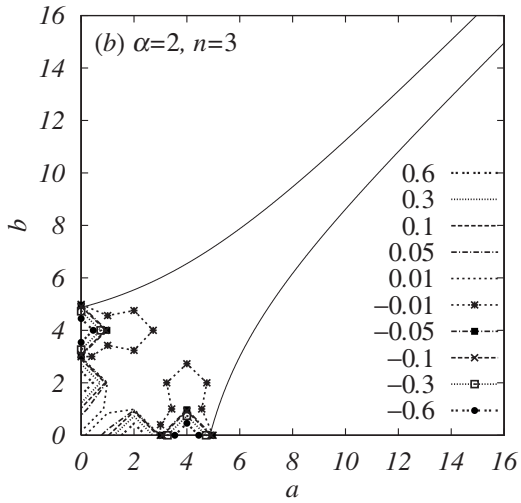


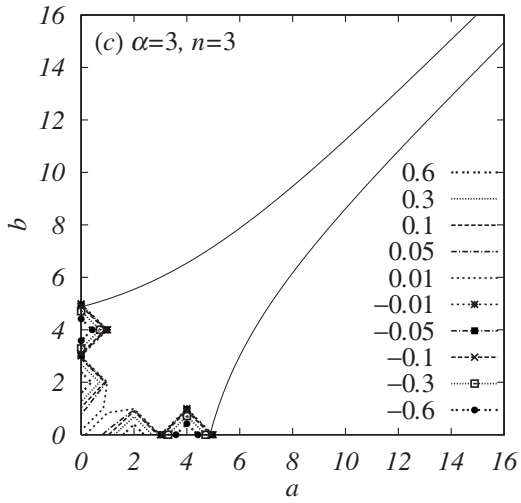


FIG. 3. Contour plots of coarse-grained triad transfer functions $T_\alpha^Q(n|a,b)$ normalized by $\eta_\alpha$ at the beginning of the EIR ($n=3$) for (a) $\alpha=1$, (b) $\alpha=2$, and (c) $\alpha=3$.

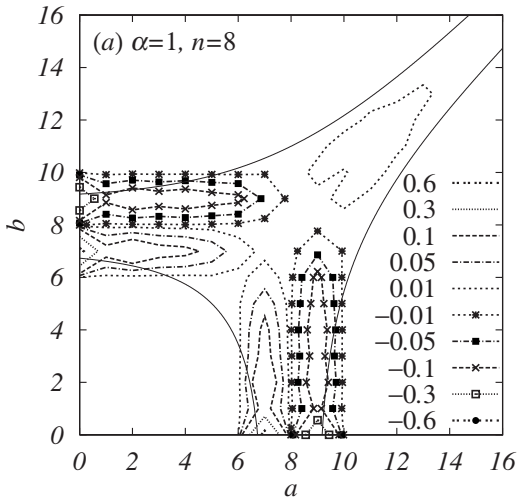


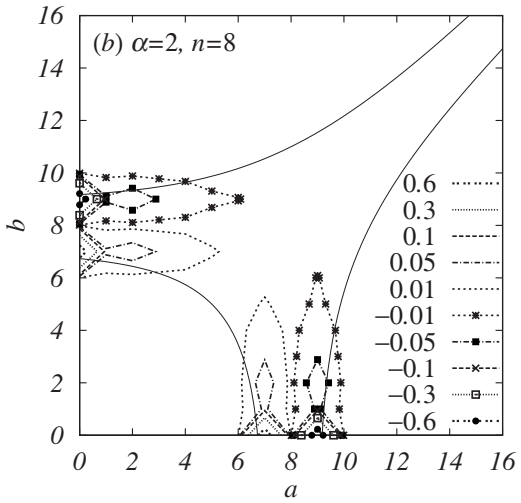


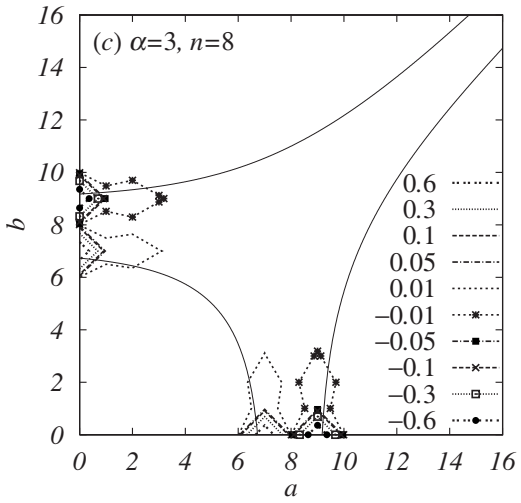


FIG. 4. Contour plots of coarse-grained triad transfer functions $T_\alpha^Q(n|a,b)$ normalized by $\eta_\alpha$ in the middle of the EIR ($n=8$) for (a) $\alpha=1$, (b) $\alpha=2$, and (c) $\alpha=3$.

fixed. Thus, the contribution from more local interactions is significant for smaller $\alpha$ systems.

To describe these observations in more detail, we show the values of $T_\alpha^Q(n|a,b)$ for specific combinations of the three shells as nonlocal interactions (0,9,10) in Table I and as local interactions (8,9,10) in Table II. The detailed balance equation $T_\alpha^Q(n|a,b)+T_\alpha^Q(a|b,n)+T_\alpha^Q(b|n,a)=0$ is satisfied accurately for both cases. Most of the enstrophy transfer occurred between the two modes $(n,a)$ or $(n,b)$ with $n \simeq a(b) \gg b(a)$, irrespective of $\alpha$. In this sense, the local en-

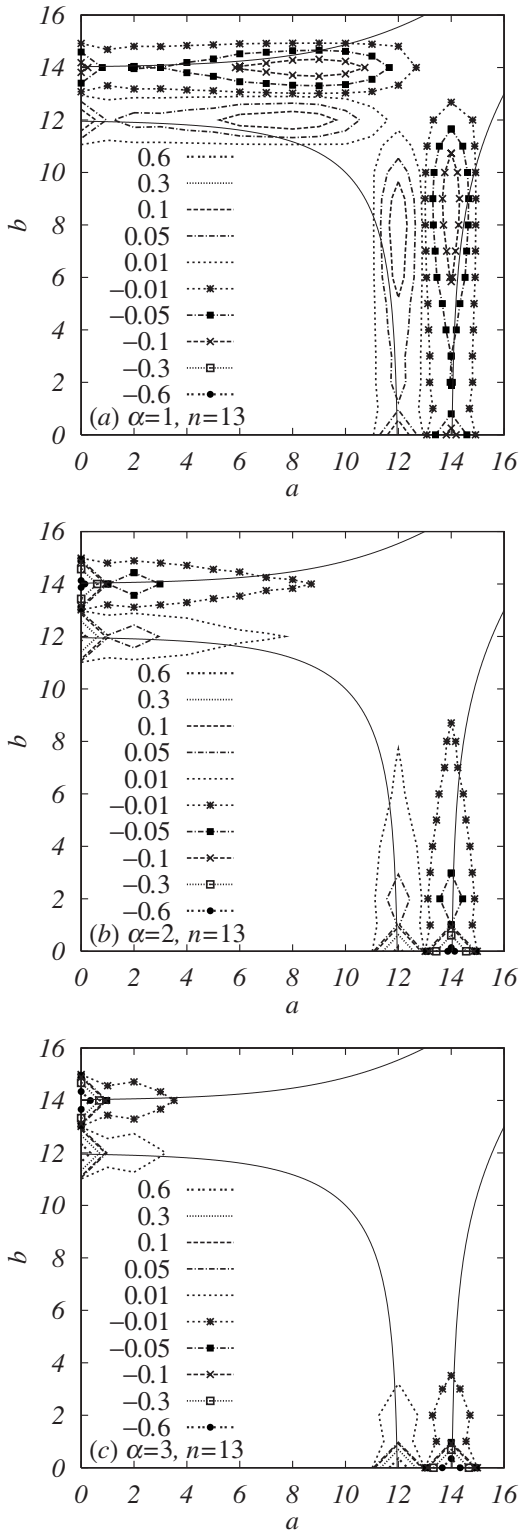


FIG. 5. Contour plots of coarse-grained triad transfer functions $T_\alpha^Q(n|a,b)$ normalized by $\eta_\alpha$ near the dissipation range ($n=13$) for (a) $\alpha=1$, (b) $\alpha=2$, and (c) $\alpha=3$.

strophy transfer is caused by the nonlocal triad interactions, as reported previously for 2D NS turbulence [8,9]. However, the amount of transfer via the nonlocal interactions is more pronounced when $\alpha>2$ than when $\alpha<2$. In addition, the amount of enstrophy transfer between the local interactions

TABLE I. Detailed balance of triad enstrophy transfer function normalized by $\eta_\alpha$ $[T_\alpha^Q(n|a,b)/\eta_\alpha]$ for a nonlocal interaction containing the forcing scale shell (0).

| | (10\|9,0) | (9\|0,10) | (0\|10,9) |
|---|---|---|---|
| $\alpha=1$ | $4.195\times10^{-1}$ | $-4.199\times10^{-1}$ | $0.004\times10^{-1}$ |
| $\alpha=2$ | $7.524\times10^{-1}$ | $-7.524\times10^{-1}$ | 0.000 |
| $\alpha=3$ | $9.283\times10^{-1}$ | $-9.283\times10^{-1}$ | 0.000 |

(8,9,10) is more significant when $\alpha=1$ than for the other cases, as shown in Table II, which clarifies observation 3.

### C. Behavior of the enstrophy transfer fluxes

Since the detailed balance equation is satisfied for $T_\alpha^Q(n|a,b)$ as well as $T_\alpha^Q(k|l,m)$, the transfer flux function $\Lambda_\alpha(n)$ given by Eq. (28) can also be decomposed into two components as

$$\Lambda_\alpha(n) = \Lambda_\alpha^+(n) + \Lambda_\alpha^-(n), \tag{29}$$

where the functions $\Lambda_\alpha^+(n)$ and $\Lambda_\alpha^-(n)$ are defined by

$$\Lambda_\alpha^+(n) \equiv \frac{1}{2}\sum_{n'=n+1}^{N_c}\sum_{a=0}^{n}\sum_{b=0}^{n} T_\alpha^Q(n'|a,b), \tag{30}$$

$$\Lambda_\alpha^-(n) \equiv -\frac{1}{2}\sum_{n'=0}^{n}\sum_{a=n+1}^{N_c}\sum_{b=n+1}^{N_c} T_\alpha^Q(n'|a,b). \tag{31}$$

These are the coarse-grained forms of Eqs. (22) and (23) represented by the shell indices. Figure 6 shows curves for (a) $\Lambda_\alpha^+(n)$ and (b) $\Lambda_\alpha^-(n)$ normalized by $\eta_\alpha$. Here, $\Lambda_\alpha^+(n)$ positively contributes to the total transfer flux; $\Lambda_\alpha^-(n)$ has negative values over the EIR, irrespective of $\alpha$, although the degree of the negative contribution differs with $\alpha$. This fact suggests that the net enstrophy input at $<n'$ by $\Lambda_\alpha^-(n)$ contributes to the enstrophy inverse cascade, providing clear evidence of a simultaneous enstrophy transfer toward scales larger and smaller than $n$; this is expected from both the Fjørtoft theorem [23] and a similar theorem developed by Merilees and Warn [24]. The enstrophy transfer by $\Lambda_\alpha^-$ toward larger scales is more pronounced as $\alpha$ decreases. The magnitude of $\Lambda_\alpha^+(n)$ in the EIR is three times that of $-\Lambda_\alpha^-(n)$ when $\alpha=1$. However, the total enstrophy transfer fluxes for $\alpha=2$ and 3 are dominated by $\Lambda_\alpha^+(n)$, i.e., $|\Lambda_\alpha^+(n)| \gg |\Lambda_\alpha^-(n)|$, as expected from Eqs. (16)–(18) with $T_\alpha^Q(n|a,b)\simeq 0$ for $a\simeq b$ [5]. This observation is in sharp contrast to the $\alpha=1$ system

TABLE II. Detailed balance of triad enstrophy transfer function normalized by $\eta_\alpha$ $[T_\alpha^Q(n|a,b)/\eta_\alpha]$ for a local interaction.

| | (10\|9,8) | (9\|8,10) | (8\|10,9) |
|---|---|---|---|
| $\alpha=1$ | $2.990\times10^{-2}$ | $-4.718\times10^{-2}$ | $1.728\times10^{-2}$ |
| $\alpha=2$ | $1.312\times10^{-3}$ | $-1.818\times10^{-3}$ | $0.506\times10^{-3}$ |
| $\alpha=3$ | $4.003\times10^{-5}$ | $-5.735\times10^{-5}$ | $1.732\times10^{-5}$ |

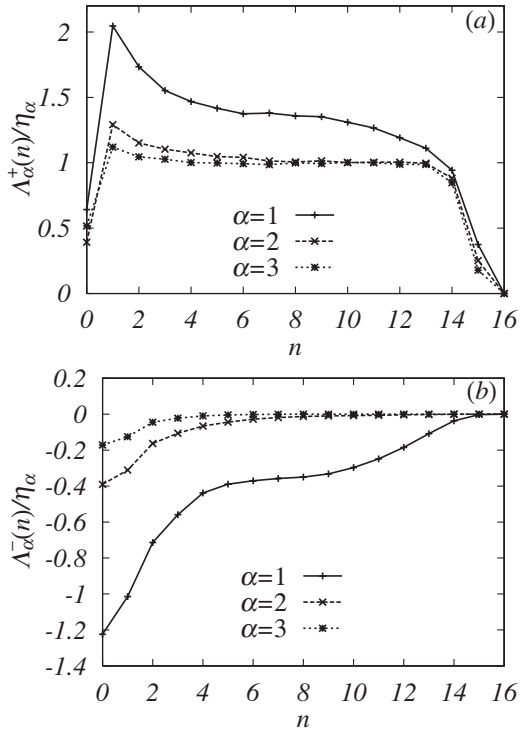


FIG. 6. Variations of the decomposed parts of the enstrophy transfer fluxes normalized by the enstrophy dissipation rate $\eta_\alpha$ as (a) $\Lambda_\alpha^+(n)$ and (b) $\Lambda_\alpha^-(n)$ against the shell index $n$ for $\alpha=1$, 2, and 3.

and to the energy transfer in 3D NS turbulence [25], in which the decomposed energy transfer fluxes, such as Eq. (29), are both positive and have similar degrees of contribution.

Let us describe the behavior shown in Fig. 6 by introducing a simplified model for $T_\alpha^Q(k|l,m)$ following the discussion of Maltrud and Vallis [8]. Assume that $T_\alpha^Q(k|l,m)$ in the EIR of $k$ can be represented by a step function in $l$ space and a constant in $m$ space as

$$T_\alpha^Q(k|l,m)=\begin{cases} S_\alpha & (k-\Delta\leqslant l\leqslant k, 0\leqslant m\leqslant \delta_\alpha), \\ -S_\alpha & (k\leqslant l\leqslant k+\Delta, 0\leqslant m\leqslant \delta_\alpha), \\ 0 & (l<k-\Delta, l>k+\Delta, \delta_\alpha<m\leqslant l), \end{cases} \tag{32}$$

where the constants $S_\alpha$ and $\delta_\alpha$ represent parameters for the amplitude and width, respectively, of the triad transfer function in $m$ space, and are independent of $k$ but dependent on $\alpha$. Suppose that the width $\Delta$ in $l$ space is independent of $\alpha$ and $k$ with $\Delta\leqslant\delta_\alpha\ll l$. This is due to the assumption that we are evaluating contributions to the enstrophy transfer fluxes from nonlocal triad interactions with $k\sim l\gg m$. Then $\Lambda_\alpha^+(k)$ can be estimated by replacing the sums in Eq. (22) with integrals as

$$\begin{aligned}\Lambda_\alpha^+(k)&=\frac{1}{2}\int_k^\infty dk'\int_0^k dl\int_0^k dm\, T_\alpha^Q(k'|l,m)\\ &\simeq\int_k^{k+\Delta}dk'\int_{k'-\Delta}^k dl\int_0^{\delta_\alpha}dm\, T_\alpha^Q(k'|l,m).\end{aligned} \tag{33}$$

Substituting Eq. (32) into Eq. (33) yields

$$\frac{\Lambda_\alpha^+(k)}{\eta_\alpha}\simeq\frac{1}{2}\hat{S}\Delta^2\delta_\alpha, \tag{34}$$

where we set $\hat{S}=S_\alpha/\eta_\alpha$, which we assume is independent of $\alpha$ for simplicity. Equation (34) suggests that $\Lambda_\alpha^+(k)/\eta_\alpha$ decreases with increasing $\alpha$ because $\delta_\alpha$ is expected to be a decreasing function of $\alpha$ based on the results of Figs. 3–5, which give the parameter $\delta_\alpha$ as a degree of the contribution from more local interactions. In a similar way, $\Lambda_\alpha^-(k)$ can be evaluated as

$$\begin{aligned}\Lambda_\alpha^-(k)&=-\frac{1}{2}\int_0^k dk'\int_k^\infty dl\int_k^\infty dm\, T_\alpha^Q(k'|l,m)\\ &=-\int_0^k dk'\int_k^\infty dl\int_l^\infty dm\frac{l^{-\alpha}-m^{-\alpha}}{m^{-\alpha}-k'^{-\alpha}}T_\alpha^Q(l|m,k')\\ &=-\int_k^\infty dk'\int_{k'}^\infty dl\int_0^k dm\frac{k'^{-\alpha}-l^{-\alpha}}{l^{-\alpha}-m^{-\alpha}}T_\alpha^Q(k'|l,m),\end{aligned} \tag{35}$$

where the relation (16) is used to derive the second equality. By substituting Eq. (32) into Eq. (35), the condition $m\ll l\sim k'$ leads to

$$\Lambda_\alpha^-(k)\simeq S_\alpha\int_k^\infty dk'\int_{k'}^{k'+\Delta}dl\int_0^{\delta_\alpha}dm\, m^\alpha(l^{-\alpha}-k'^{-\alpha}). \tag{36}$$

Integrating Eq. (36) with the condition $\Delta\ll k'$ yields

$$\frac{\Lambda_\alpha^-(k)}{\eta_\alpha}\simeq-\frac{1}{2(\alpha+1)}\hat{S}\Delta^2\delta_\alpha\left(\frac{\delta_\alpha}{k}\right)^\alpha. \tag{37}$$

The resulting equation (37) suggests the two important points:

(1) $\Lambda_\alpha^-(k)$ is negative, as shown in the DNS results.

(2) The amplitude of $\Lambda_\alpha^-(k)$ is much less than that of $\Lambda_\alpha^+(k)$ if $\delta_\alpha\ll k$ with $\alpha>0$.

The relative importance of the enstrophy inverse cascade due to $\Lambda_\alpha^-$ is more pronounced for smaller $\alpha$ turbulence; this occurs because the amplitude of $\Lambda_\alpha^-(k)$ grows sharply with decreasing $\alpha$ due to the $\alpha$ dependence of the factor $(\delta_\alpha/k)^\alpha$ that appears in Eq. (37). Thus, the present model suggests that the "backscatter" of enstrophy for $\alpha=1$, more than that of the other cases shown in Fig. 6, originates from the increase in the more local interaction contributions with decreasing $\alpha$, which is consistent with the present DNS results.

### D. Fractional contribution to the enstrophy transfer fluxes

To quantify the contribution to the enstrophy transfer flux of $\alpha$ turbulence from local and nonlocal interactions, we introduced a parameter to characterize the shape of the triangle composed of the triad interactions with the wave vectors $\mathbf{k}+\mathbf{l}+\mathbf{m}=\mathbf{0}$. We defined the function $W_\alpha(s,n)$ as

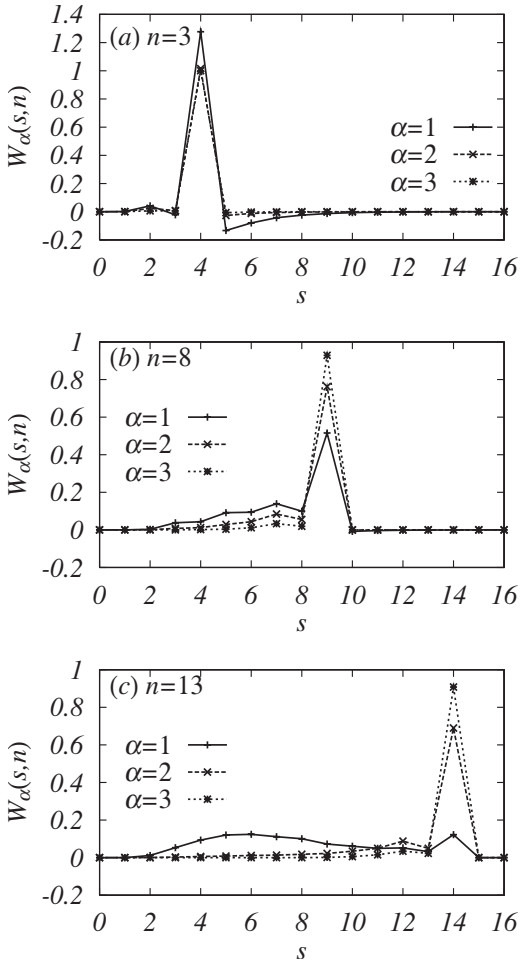


FIG. 7. Comparison of the fractional contributions to the enstrophy transfer flux among the $\alpha=1$, 2, and 3 cases at the scale (a) $n=3$, (b) $n=8$, and (c) $n=13$.

$$\frac{\Lambda_\alpha(n)}{\eta_\alpha} = \sum_{s=0}^{N_c} W_\alpha(s,n), \tag{38}$$

where $s$ is a parameter that plays the same role as the scale disparity parameter [5,25,28] defined by

$$\lambda^s \equiv \frac{\max(k_n,l_a,m_b)}{\min(k_n,l_a,m_b)}, \tag{39}$$

or equivalently

$$s \equiv \max(n,a,b) - \min(n,a,b). \tag{40}$$

The function $W_\alpha(s,n)$ is the fractional contribution to the enstrophy transfer flux from the triad interactions with the shape of the triangle categorized by $s$. $W_\alpha(s,n)$ at larger $s$ ranges represents the contribution from more nonlocal interactions, while the contribution from more local interactions is characterized by the behavior at smaller $s$ ranges. Figure 7 shows the behavior of $W_\alpha(s,n)$ against $s$ with the following fixed scales in the EIR: (a) $n=3$, (b) $n=8$, and (c) $n=13$. $W_\alpha(s,n)$ has a peak at $s_p=n+1$, irrespective of $\alpha$, and the peak intensity varies with the value of $\alpha$. This sharp peak is caused by the triad transfer function with the interacting forcing scales as $T_\alpha(n|0,n+1)$. As $n$ increases, the peak intensity $W_\alpha(s_p,n)$ decreases and the contribution from more local interactions as $s<s_p$ becomes more positive. This trend is more significant for the smaller $\alpha$ case. The contribution from more nonlocal interactions as $s>s_p$ leads to the negative value of $W_\alpha(s,n)$, which originates from the contribution of $W_\alpha^-(s,n)$ [Eq. (42)], as discussed in the next paragraph. Therefore, we conclude that the interacting scales that contribute to the enstrophy transfer flux for $\alpha<2$ are relatively more local than when $\alpha\geqslant 2$, although the contribution from nonlocal triad interactions specified by $s=s_p$ is most significant in the EIR, irrespective of $\alpha$.

To investigate the contribution from the local and nonlocal interactions discussed above in more detail, we evaluated the fractional contributions $W_\alpha^+(s,n)$ and $W_\alpha^-(s,n)$ to the components $\Lambda_\alpha^+(n)$ and $\Lambda_\alpha^-(n)$ and determined their behavior for different $\alpha$ and $n$ separately. The functions $W_\alpha^+(s,n)$ and $W_\alpha^-(s,n)$ are defined by

$$\frac{\Lambda_\alpha^+(n)}{\eta_\alpha} = \sum_{s=0}^{N_c} W_\alpha^+(s,n), \tag{41}$$

$$\frac{\Lambda_\alpha^-(n)}{\eta_\alpha} = \sum_{s=0}^{N_c} W_\alpha^-(s,n). \tag{42}$$

The equality $W_\alpha(s,n)=W_\alpha^+(s,n)+W_\alpha^-(s,n)$ should be satisfied from the definition of $W_\alpha(s,n)$. Figure 8 shows $W_\alpha^+(s,n)$ in the EIR of $n$ against the scale disparity parameter $s$ for (a) $\alpha=1$, (b) $\alpha=2$, and (c) $\alpha=3$. A single peak occurs for each $n$ at $s=n+1(=s_p)$, which comes from the nonlocal triad interactions via the forcing scale shells, as shown in Fig. 7. Although the values of $W_\alpha^+(s_p,n)$ for $\alpha=2$ and 3 are almost the same for different $n$, as long as $n$ is in the EIR, the case of $\alpha=1$ gives a peak value that gradually decreases with increasing $n$, where the contribution from more local interactions in the range $3<s<7$ grows. These trends are almost the same as the behavior of $W_\alpha(s,n)$ because $W_\alpha(s,n)$ is dominated by $W_\alpha^+(s,n)$, especially when $\alpha=2$ and 3.

Figure 9 shows $-W_\alpha^-(s,n)$ plotted on a semilogarithmic scale for (a) $\alpha=1$, (b) $\alpha=2$, and (c) $\alpha=3$. $W_\alpha^-(s,n)$ has negative values over the entire range of $s$, irrespective of $\alpha$, and its amplitude decreases with increasing $\alpha$, where $|W_\alpha^-(s,n)|$ is much less than $W_\alpha^+(s,n)$ for $\alpha=2$ and 3. This fact is expected from the results of Fig. 6(b) and the analysis of the transfer model discussed in the previous section. The negative contribution of $W_\alpha^-(s,n)$ to the total enstrophy transfer flux is more significant for $\alpha=1$ in the range $2<s<6$ than when $\alpha=2$ and 3. The curves for $\alpha=1$ have peaks around $s=4$ and are almost superimposed, irrespective of $n$ in the EIR. This implies that the enstrophy transfer toward scales larger than $k_n^{-1}$ with $n=s_p$ occurs via more local interactions. However, this negative contribution is also canceled by the excess forward transfer by $W_1^+(s,n)$, which has positive values greater than $-W_1^-(s,n)$ in the range $2<s<6$. These observations combined with the results of Fig. 8 clearly suggest that the contribution to the enstrophy transfer toward smaller scales from more nonlocal interactions dominates at the end of the

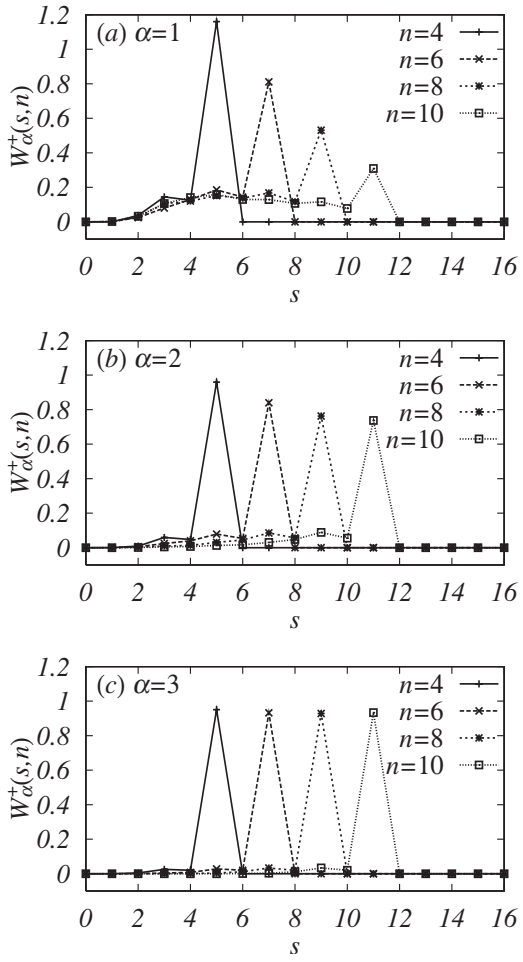


FIG. 8. Comparison of the fractional contributions to the enstrophy transfer flux $\Lambda^+_\alpha(n)$ at the scales of the EIR for (a) $\alpha=1$, (b) $\alpha=2$, and (c) $\alpha=3$. The scales $n=4-10$ correspond to the range in which the enstrophy spectrum $Q_\alpha(k)$ obeys the form (5) with (6).

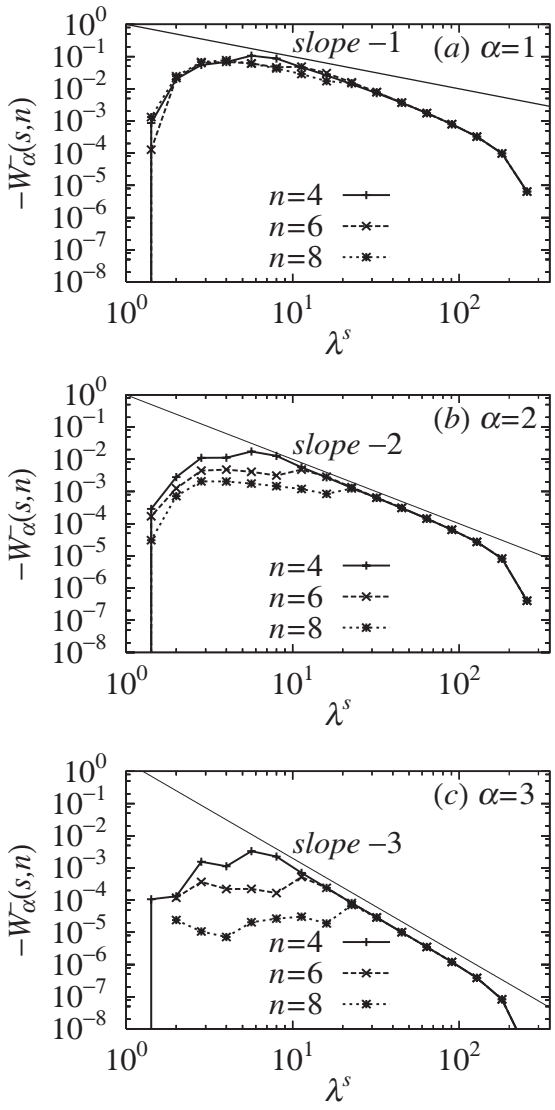


FIG. 9. Comparison of the fractional contributions to the enstrophy transfer flux $-\Lambda^-_\alpha(n)$ at the scales of the EIR for (a) $\alpha=1$, (b) $\alpha=2$, and (c) $\alpha=3$.

EIR scales, manifesting the apparent evidence of enstrophy transfer governed by the large-scale straining motions. This trend becomes less significant as $\alpha$ decreases, when the contribution from more local interactions to the enstrophy transfer grows in both directions for the larger and smaller scales.

$|W^-_\alpha(s,n)|$ follows the power-law decay as $|W^-_\alpha(s,n)| \sim (\lambda^s)^{-\gamma(\alpha)}$ when $s>s_p$, irrespective of $n$. A rough estimation of this scaling behavior follows based on the model transfer function [Eq. (32)]. Evaluating the integral of Eq. (36) in terms of the scale disparity parameter $y \equiv k/\delta_\alpha (=\lambda^s)$ yields

$$\frac{\Lambda^-_\alpha(k')}{\eta_\alpha} \simeq -\frac{\delta_\alpha \Delta^2 \alpha}{2(\alpha+1)} \hat{S} \int_{y'}^{\infty} \frac{dy}{y} y^{-\alpha} = \int_{y'}^{\infty} \frac{dy}{y} W^-_\alpha(y). \quad (43)$$

Thus, we obtain a scaling in the form of $W^-_\alpha(y) \propto -y^{-\alpha}$, i.e., $\gamma(\alpha)=\alpha$. This scaling is also compared to the numerical results in Fig. 9, which indicates that the above prediction works well for $\alpha \geqslant 2$. The apparent difference between the model predictions and DNS results for $\alpha=1$ is due to the simplification of the model using Eq. (32), which approximates the contribution from more local interactions by $\delta_\alpha$. Further analysis using the spectral theory given in [8,27,28] may be required to determine the detailed behavior of $W^-_\alpha(y)$. This issue is beyond the scope of the present paper because the contributions from the larger $s$ range of $W^-_\alpha(y)$ are not important compared to those from the range $2<s<6$.

## IV. DISCUSSION

Using the characteristics of the enstrophy transfer obtained from the present simulations, we examined the validity of the phenomenological scaling theory, which represents the local and nonlocal transition at $\alpha=2$ proposed in [16].

Recall that the key idea for deriving Eqs. (5) and (6) was to incorporate nonlocal effects into the transfer time at the scale $k^{-1}$ evaluated by Eq. (7) as $\tau_\alpha(k) \equiv \omega_\alpha(k)^{-1} = [\int_0^k k'^{4-2\alpha} Q_\alpha(k') dk']^{-1/2}$ instead of adopting $\tau_\alpha(k) \sim [k^{5-2\alpha} Q_\alpha(k)]^{-1/2}$, which leads to the KLB scaling law (3) with $\eta_\alpha \sim k Q_\alpha(k)/\tau_\alpha(k)$. The form (7) implies that the large-scale straining effects at $k'<k$ are represented by the scale-

dependent rate of shear $\omega_\alpha(k)$ $[\omega_\alpha(\infty) \sim \langle(\partial_1 u_1)^2\rangle^{1/2}]$. In this sense, the derived spectral form (5) implicitly includes the effects of the enstrophy transfer due to nonlocal interactions. The resulting DNS analysis suggests that the enstrophy transfer for $\alpha=2$ and 3 predominantly occurs via nonlocal interactions containing the forcing scales in the middle of the EIR. Therefore, the evaluation of the transfer time using Eq. (7) is more plausible for $\alpha \geqslant 2$. For SQG turbulence, i.e., $\alpha=1$, we observed in Figs. 7 and 8 that, although $W_1(s,n)$ is almost the same as the cases for $\alpha=2$ and 3 when $n=4$, the contribution from more local interactions is comparable to those from nonlocal interactions when $n=8$, i.e., $\Sigma_{s=0}^{8} W_1(s,8) \simeq \Sigma_{s=9}^{N_c} W_1(s,8)$. As $n$ increases up to $n=13$, the contribution from nonlocal interactions significantly decreases. Thus the enstrophy transfer of SQG turbulence in the EIR is characterized by the increase (decrease) of contribution from local (nonlocal) interactions with decrease of scale. This fact is indeed consistent with the success of the unified scaling theory for $\alpha<2$ shown in Fig. 1 because the scaling form (5) allows us to have large-scale corrections to the KLB scaling due to the nonlocal effects in the EIR scale. If the EIR is much wider than the present DNS at $\alpha=1$, we expect the contributions to the enstrophy transfer from nonlocal interactions to decrease significantly with the scale. Then the contributions from more local interactions can predominate the transfer dynamics in the EIR, implying that the power-law form predicted by the KLB scaling (3) can be asymptotically observed in the smaller EIR scales. To resolve this issue, we require further DNSs with a much finer resolution to realize a state in which classical arguments are asymptotically correct.

Another notable finding observed in the SQG turbulence is that the contribution of $\Lambda_\alpha^-(k)$, which causes the enstrophy inverse cascade, to the total enstrophy transfer flux is more significant when $\alpha=1$. The local interaction contributions also dominated $\Lambda_\alpha^-(k)$. This is in sharp contrast to $\alpha \geqslant 2$, and manifests the complicated transfer dynamics not considered in the phenomenological argument on dimensional grounds. The coexistence of forward and backward enstrophy transfers via local interactions implies that the interacting dynamics between small-scale structures with similar characteristic scales as the EIR, such as the vortical structure shown in [16], play an important role in the transfer dynamics of SQG turbulence in physical space; however, the passive nature of the scalar $q$ governed by the large-scale straining motions also introduces a significant transfer process. A more precise analysis of the enstrophy transfer in physical space, such as that performed when investigating the local transfer flux in 2D NS turbulence [29], is needed.

The above implication also raises a fundamental problem about how the vortical structures and their collective dynamics in SQG turbulence are different from those of 2D NS turbulence. It would be interesting to clarify the features of population dynamics of vortical structures in SQG turbulence and to observe the difference between population dynamics of coherent vortices in 2D NS turbulence [30,31] and that in SQG turbulence. Some specific characteristics of the interacting scales between vortices have been discussed in [13,17]; the interacting scales of SQG vortices were more local than those in the 2D NS case due to the relation (2).

## V. SUMMARY

We discussed the local and nonlocal characteristics of the triad enstrophy transfer in $\alpha$ turbulence by investigating the behavior of several statistical quantities such as the triad enstrophy transfer functions obtained from DNSs. The contributions to the total enstrophy transfer from more local triad interactions were more significant when $\alpha=1$ than for systems with $\alpha=2$ and 3. We demonstrated that nonlocal interactions containing the forcing scales were more predominant in the total enstrophy transfer for larger $\alpha$ systems. This result encourages us to explain the local and nonlocal transition of $\alpha$ turbulence at $\alpha=2$ in terms of the different characteristics of the interacting scales in wave-number space, although the triad transfer function from DNS does not show a drastic transition at $\alpha=2$.

The enstrophy transfer fluxes and their fractional contributions were also examined to quantify the degree of contribution from the local and nonlocal scale interactions. We observed that the nonlocal interactions predominantly contributed to the total enstrophy flux, irrespective of $\alpha$, at scales ranging from the beginning to the middle of the EIR; however, their contributions decreased with $\alpha$ at the end of the EIR, as shown for the triad transfer function. More local interactions significantly contributed to both the inverse and direct enstrophy cascades when $\alpha=1$. An enstrophy transfer toward larger scales was also observed for $\alpha \geqslant 2$, although the amount of enstrophy transfer was negligibly small compared to transfer from the enstrophy direct cascade via nonlocal interactions. These features were discussed using a simple triad transfer model, and we demonstrated that more backscatter of enstrophy occurred for the smaller $\alpha$ case due to the increased contributions from more local interactions.

The unique nature of the enstrophy cascade in SQG turbulence ($\alpha=1$) emerged from the present analysis. Coexisting small-scale vortical structures and large-scale straining motions in the scalar field $q$ [16] were observed, consistent with the enstrophy transfer characteristics in wave-number space described in the present paper. It would be desirable to obtain more insight into the enstrophy transfer toward smaller scales using quantities in physical space when $\alpha=1$. This is left to a future study.

## ACKNOWLEDGMENTS

T.W. was supported by a Grant-in-Aid for Scientific Research No. 17760139 from the Ministry of Education, Culture, Sports, Science and Technology of Japan (MEXT). T.I. was supported by a Grant-in-Aid for Scientific Research No. 18540433 from the Japanese Society for the Promotion of Science and the 21st Century COE Program of Origin and Evolution of Planetary Systems in the MEXT.

[1] A. N. Kolmogorov, Dokl. Akad. Nauk SSSR **30**, 9 (1941).
[2] R. H. Kraichnan, Phys. Fluids **10**, 1417 (1967).
[3] C. E. Leith, Phys. Fluids **11**, 671 (1968).
[4] G. K. Batchelor, Phys. Fluids **12**, II-233 (1969).
[5] R. H. Kraichnan, J. Fluid Mech. **47**, 525 (1971).
[6] J. C. Bowman, J. Fluid Mech. **306**, 167 (1996).
[7] K. Ohkitani, Phys. Fluids A **2**, 1529 (1990).
[8] M. E. Maltrud and G. K. Vallis, Phys. Fluids A **5**, 1760 (1993).
[9] K. G. Oetzel and G. K. Vallis, Phys. Fluids **9**, 2991 (1997).
[10] V. Borue, Phys. Rev. Lett. **71**, 3967 (1993).
[11] J.-P. Laval, B. Dubrelle, and S. Nazarenko, Phys. Rev. Lett. **83**, 4061 (1999).
[12] Y. Kaneda and T. Ishihara, Phys. Fluids **13**, 1431 (2001).
[13] R. T. Pierrehumbert, I. M. Held, and K. L. Swanson, Chaos, Solitons Fractals **4**, 1111 (1994).
[14] N. Schorghofer, Phys. Rev. E **61**, 6572 (2000).
[15] K. S. Smith, G. Boccaletti, C. C. Henning, I. Marinov, C. Y. Tam, I. M. Held, and G. K. Vallis, J. Fluid Mech. **469**, 13 (2002).
[16] T. Watanabe and T. Iwayama, J. Phys. Soc. Jpn. **73**, 3319 (2004).
[17] I. M. Held, R. T. Pierrehumbert, S. T. Garner, and K. L. Swanson, J. Fluid Mech. **282**, 1 (1995).
[18] K. Ohkitani and M. Yamada, Phys. Fluids **9**, 876 (1997).
[19] T. Watanabe, H. Fujisaka, and T. Iwayama, Phys. Rev. E **55**, 5575 (1997).
[20] T. Watanabe, T. Iwayama, and H. Fujisaka, Phys. Rev. E **57**, 1636 (1998).
[21] T. Iwayama, T. Watanabe, and T. G. Shepherd, J. Phys. Soc. Jpn. **70**, 376 (2001).
[22] T. Iwayama, T. G. Shepherd, and T. Watanabe, J. Fluid Mech. **456**, 183 (2002).
[23] R. Fjørtoft, Tellus **5**, 225 (1953).
[24] P. E. Merilees and H. Warn, J. Fluid Mech. **69**, 625 (1975).
[25] Y. Zhou, Phys. Fluids A **5**, 2511 (1993).
[26] J. A. Domaradzki and D. Carati, Phys. Fluids **19**, 085112 (2007).
[27] K. Ohkitani and S. Kida, Phys. Fluids A **4**, 794 (1992).
[28] T. Gotoh and T. Watanabe, J. Turbul. **6**, 1 (2005).
[29] S. Chen, R. E. Ecke, G. L. Eyink, X. Wang, and Z. Xiao, Phys. Rev. Lett. **91**, 214501 (2003).
[30] G. F. Carnevale, J. C. McWilliams, Y. Pomeau, J. B. Weiss, and W. R. Young, Phys. Rev. Lett. **66**, 2735 (1991).
[31] T. Iwayama and H. Okamoto, Prog. Theor. Phys. **96**, 1061 (1996).
[32] The system for $\alpha=1$ is called the surface quasigeostrophic (SQG) equation, which describes the motion of the surface temperature field in a stratified fluid with rotation [17,18]. The system for $\alpha=2$ corresponds to the vorticity equation derived from the 2D NS equations, where $q$ is the vorticity. The system for $\alpha=-2$ is equivalent to the asymptotic model of the Charney-Hasegawa-Mima equation [19–22], one of the fundamental equations in geophysical fluid dynamics or plasma physics.